ACOUSTICS 2012

Seafloor characterization by means of nonlinear multi-frequency generation

L. Di Marcoberardino, J. Marchal and P. Cervenka

Institute Jean Le Rond d'Alembert, 2 place de la gare de Ceinture, 78210 Saint Cyr L'Ecole, France
lucilla.dimarcoberardino@idasc.cnr.it

In the underwater context, it is known that the frequency diversity provides essential information to derive the nature of the seafloor. Actually, the information gathered from each single frequency gives a complementary picture of a particular environment. This presentation deals with the realization of a multi-frequency acoustic surveying tool based on the saturation effect. The transmitter is fed with a high-power single tone-burst: numerous harmonic waves are created by non linear interactions along the propagation. The source is unique in time and space so that the multi-frequency responses are inherently perfectly matched. The receiver is a rectangular multi-element broadband array realized for measurements in the sea environment. Seabed characterization measurements were made in the bay of Brest. First results of sediment backscatter response and seafloor images are presented.

1 Introduction

Classical acoustical surveying systems gather data about the seafloor usually on a narrow frequency bandwidth: a single system does not provide frequency diversity in the collected acoustic backscattered intensities. Gathering data at different frequencies would be an interesting asset for sea floor characterization. Geological surveys, industrial monitoring of underwater structures and environment protection are applications that are potentially concerned. For example, the interest of the multi-frequency approach has been put in evidence in a study about the capability to detect sunken oil slicks [1]. Results showed that high frequencies sources revealed the presence of flat superficial spots (specular reflection, no backscattered energy) whereas low frequency responses show the underlying substrate (transmission through the thin layer of oil). The combination of all acquired information gave the possibility to deduce the oil slicks presence. At the present time, gathering multi-frequency information implies using several different systems. Consequently, the collected data are not perfectly matched in time and space, and the fusion is problematic.

This study is related to the feasibility of an original system that takes advantage of nonlinear propagation to achieve a multifrequency source. The principle is to generate a harmonic pulse with sufficient energy so that the saturation phenomenon emerges [2]. As a result, a single source generates a whole set of beams at the harmonic frequencies, and all these beams are perfectly superposed both in time and in space.

In the medical domain, the second harmonic that is generated by the nonlinearity of the propagation is already a classical technique to improve the resolution of the echographic acoustical images [3]. On the other hand in the underwater acoustic domain, the nonlinearity of the propagation is perceived as a penalizing effect, but for the parametric transmitter application. Saturation implies indeed a lowering of the transmitters' efficiency [2]. When increasing the transmitted power, part of the acoustical energy is transferred along the propagation to higher harmonic components. It leads to a saturation effect on the fundamental frequency which limits the source level that can be reached.

We present here the results of trials at sea with a sonar prototype. From a practical point of view, it is desirable that the beam patterns feature a large aperture along one dimension. Hence the difficulty was to design a transmitter that produces harmonic beams with such required geometry, while keeping sufficient source levels. The receiver was then conceived in function of the characteristics of the source. The complete chain (emission and reception) has been tested in the bay of Brest during a one-day campaign onboard the IFREMER's vessel Thalia.

A preliminary experimental investigation of saturation induced generation was performed and the resulting on-axes level and beam patterns are presented. The reception chain is then described. First sea trial results are finally displayed.

2 Nonlinear propagation

2.1 Equations

The nonlinear quadratic equation of propagation in fluids can be written as [4]:

$$\begin{aligned}\Delta\Phi - \frac{1}{c_0^2}\frac{\partial^2\Phi}{\partial t^2} - \frac{2}{c_0}\mathrm{L}\left(\frac{\partial\Phi}{\partial t}\right) \\ = \frac{1}{c_0^2}\frac{\partial}{\partial t}\left\{\left(\nabla\Phi\right)^2 + \left(\beta-1\right)\frac{1}{c_0^2}\left(\frac{\partial\Phi}{\partial t}\right)^2\right\}\end{aligned} \tag{1}$$

where $\Phi(\mathbf{r},t)$ is the acoustic potential, c_0 is the sound speed and β is the nonlinear coefficient. The left term is the operator of propagation. The right term accounts for the sources of the nonlinear phenomena. $\mathrm{L}\left(\partial\Phi/\partial t\right)$ is a linear operator that includes absorbing and dispersive effects [5]. However from a practical point of view, it is more convenient to handle the attenuation as a function of the frequency f by using the attenuation coefficient $\alpha(f)$:

$$\mathrm{L}\left(e^{j2\pi f t}\right) = \alpha\left(f\right)e^{j2\pi f t} \tag{2}$$

In the sea water, the Francois-Garrison model [6] is commonly admitted.

The observable parameters are the acoustic velocity v and pressure P that are related to the potential Φ through:

$$\begin{cases} v = \mathrm{grad}\left(\Phi\right) \\ P = -\rho_0\dfrac{\partial\Phi}{\partial t} - \dfrac{\rho_0}{2}\left[\left(\nabla\Phi\right)^2 - \dfrac{1}{c_0^2}\left(\dfrac{\partial\Phi}{\partial t}\right)^2\right]\end{cases} \tag{3}$$

(ρ_0 is the density). In the paraxial approximation, the introduction of the retarded time $t' = t - z/c_0$ (where z is the main beam axis) in Equation (1) leads to an equation similar to the KZK (Khokhlov-Zabolotskaya-Kuznetsov) equation:

$$\frac{\partial^2 P}{\partial z\partial t'} = -\mathrm{L}\left(\frac{\partial P}{\partial t}\right) + \frac{\beta}{2\rho_0 c_0^3}\frac{\partial^2\left(P^2\right)}{\partial t'^2} - \frac{c_0}{2}\Delta_\perp P \tag{4}$$

$\Delta_\perp = \partial^2/\partial x^2 + \partial^2/\partial y^2$ is a Laplacian that operates in the plane perpendicular to the beam axis.

2.2 Nonlinear characteristic distances

Taking $\tau = \omega_0 t'$, $x = Ax'$, $y = By'$ and $P = \rho_0 c_0 v_0 p$, where A and B are the dimensions of the rectangular antenna and v_0 is the velocity normal to the projector surface, Equation (4) can be expressed in the following dimensionless form:

$$\frac{\partial^2 p}{\partial z \partial \tau} = \frac{1}{L_\alpha} L'\left(\frac{\partial p}{\partial \tau}\right) + \frac{1}{L_s}\frac{\partial^2}{\partial \tau^2} p^2 - \frac{1}{4\pi L_{FA}}\frac{\partial^2 p}{\partial x'^2} - \frac{1}{4\pi L_{FB}}\frac{\partial^2 p}{\partial y'^2}. \quad (5)$$

$L_\alpha = 1/\alpha(f_0)$ is the characteristic attenuation distance, $L_S = c_0^2/\beta v_0 \omega_0$ is the shock formation distance, $L_{FA} = A^2/\lambda_0$ and $L_{FB} = B^2/\lambda_0$ are the Fraunhofer distances (λ_0 is the wavelength corresponding to the fundamental frequency f_0). $L' = L/\alpha(f_0)$ is the dimensionless attenuation propagator that simplifies into $L' = \partial^2/\partial\tau^2$ for pure fresh water.

Equation (5) is a simple model of the finite amplitude wave propagation. Three antagonist phenomena are involved: linear absorption, shock formation and diffraction. The nonlinear effect is observable only if the shock formation distance L_S is shorter than the other characteristic distances L_α and L_F. These characteristic distances are the relevant parameters to design a multi-frequency projector.

3 The multifrequency source

The parameters of the antenna are given in Table 1. The transmitting frequency is $f_0 = 100$ kHz ($\lambda_0 = 1.5$ cm): the source is made of three elements working in piston mode.

Table 1: *characteristic values of the emitter.*

Dimensions	3.1 cm × 78 cm
Aperture -3dB	24° × 0.97°
L_F	6 cm and 40 m
L_α	235 m
Sv @ 100kHz	176 dB re 1µPa/V

3.1 Experimental setup

The source has been tested in the 50m × 10m × 10m Ifremer tank (sea water). Because of the hydrophone bandwidth (Reson TC4034, 1 Hz – 500 kHz), the only measurements of the first five harmonics are reported. The power is provided by a custom E/D class amplifier that delivers up to 20 kW electrical power. The signal output by the amplifier is square shaped. Consequently, its spectral content is a combination of odd harmonics. A filter has been inserted in the matching circuit to reject all the harmonics in the electrical signal that feed the antenna down to more than −30 dB [7]. The source level at the fundamental frequency can be directly estimated from the voltage feeding the antenna and the sensitivity of the transducer that has been established with a 50W linear amplifier (see Sv Table 1). Table 2 displays the acoustic levels obtained as a function of the nominal electric power delivered by the amplifier (the global electric-acoustic efficiency of the transmitter is in the range 30%–70%). Comparing the characteristic distances in Tables 1 and 2, it appears that L_α is always much larger than L_S and L_F, so that the attenuation is never the dominant effect. On the other hand, it can be seen that diffraction and non linearity are competing effects.

Table 2. *Source levels (dB re 1 µPa rms) and shock distance in function of the applied power.*

Pe	P_0	P @ 1m	L_S
1.2 kW	221 dB	225 dB	6.9 m
5 kW	227 dB	231 dB	3.6 m
20 kW	233 dB	237 dB	1.8 m

The absolute acoustic levels obtained with the antenna are quite large. Figure 1 displays the on-axis levels obtained at the maximal available electrical power. Although the transmitter sensitivities of the rectangular transducers are penalized by their large aperture along one principal plane, the source levels are still in the range 217 dB to 235 dB re 1 µPa @ 1 m. Comparisons with a numerical estimation are shown (the pseudo-1D model used is described in [8]).

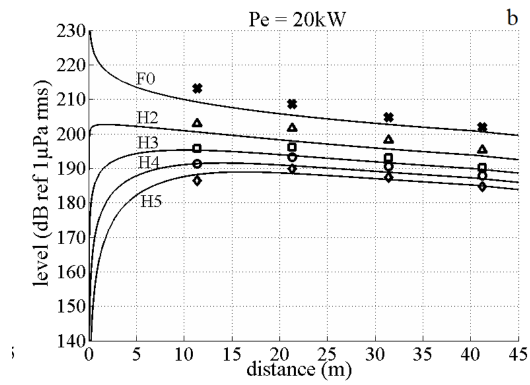

Figure 1. Harmonics level versus distance. P_e = 20 kW. Marks: measurements. Lines: pseudo-1D model.

Preliminary directivity measurements are displayed in Figure 2. The corresponding characteristic apertures are reported in Table 3. These measurements are performed in a plane that is perpendicular to the z-axis, i.e. not at a constant range. As expected, the higher is the harmonic, the narrower is the aperture. However, the beamwidth does not depend linearly on the frequency.

Table 3. Beam width of each source. Measures are related to conditions explained in figure 2.

	f_0	H2	H3	H4	H5
x-axis	29°	24°	21°	20°	19°
y-axis	1.15°	0.78°	0.66°	0.59°	0.54°

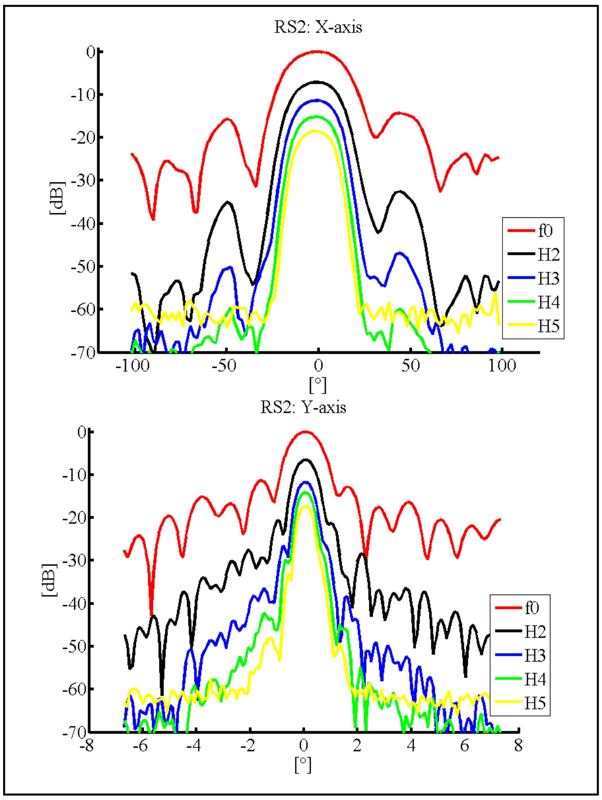

Figure 2. Directivity of the first harmonics ($z = 41$ m, $P_e = 20$ kW). Top: x-axis. Bottom: y-axis

4 The receiver

The first experimental results of the multifrequency source confirmed the feasibility of an underwater transmitter able to exploit the nonlinearity of wave propagation. Source levels were measured using a simple omni-directional hydrophone as a receiver in the tank. The next step is to test the multifrequency source at sea in order to measure backscatter indexes of different sediments. This requires designing a dedicated receiver.

The receiving antenna is a 70 cm long linear array that provides a large aperture along one dimension and a narrow beamwidth along the other dimension. The array is made of 24 piezoelectric rectangular elements (2.8 mm × 45 mm × 2.1 mm) disposed over two parallel lines. The resonance of these elements is at 900 kHz, the purpose being to obtain a wide band receiver (100 kHz - 500 kHz). The main characteristics of the receiving antenna are reported in Table 4. The elements are connected to three acquisition cards NI-DAC 6366 via pre-amplifiers (+34 dB). The sampling frequency of the 24 signals is 2 MHz.

The division of the linear antenna into several elements enables to tune the beam patterns at post-processing: the received signal can be combined so as to keep almost the same beamwidth for all the harmonic frequencies. This antenna design gives also the bathymetry capability by means of interferometry.

Table 4: characteristic parameters of the receiver.

Dimensions	3.5 cm x 67cm	
Frequency	100 kHz	500 kHz
Aperture (-3dB)	>100° × 17°	54° × 3°
L_F	0.5 mm and 0.14 m	2.6 mm and 0.7 m
S_H (dB re 1V/ µPa)	-212 dB	-189 dB

5 First sea trials

The complete system has been tested during a one-day sea trial in the bay of Brest on the IFREMER's ship Thalia. Fig. 3 shows both the source and the receiver positioned together on a mechanical arm at starboard of the vessel. Both antennas are slanted 45° from the vertical. Well documented areas featuring different kinds of sediments were sounded.

Fig. 4 displays the waterfall of four harmonic's responses for a sequence of pings. Harmonics are sorted by using a boxcar filter in the frequency domain. Levels are corrected with the calibrated levels of the multi-frequency source and with a linear transmission loss correction for the return way.

Fig. 5 displays the mean energy received for each harmonic. The abscissa is the ratio range over depth. The only first part of signals is taken into account, i.e., before the onset of the double reflection that occurs at $r/h \geq 2$. Although not yet fully processed, it can be readily observed that harmonic responses have different shapes. A thorough analysis of these data will require taking into account the incident angles estimated with bathymetric methods.

6 Conclusion

The feasibility of a new underwater source able to exploit higher harmonics generated by the nonlinear propagation has been studied and validated. The most challenging issue is the harmonic source levels that can be expected with elongated rectangular antennas, i.e., whose beam pattern is quite large in one plane. To this respect, the beam characteristics measured with the source are very encouraging because the geometry and central frequency of this antenna are relevant for surveying tasks. A receiving antenna was designed and built for sea trials purposes. Backscattered echoes from the seafloor were recorded at sea. These records still need a thorough analysis to extract the expected differential frequency signatures versus the angle of view of the various sediments. To this end, additional post-processing for taking into account the relief of the surveyed area must be done.

Figure 3. Multifrequency source and wideband receiver used during the sea trials in the bay of Brest.

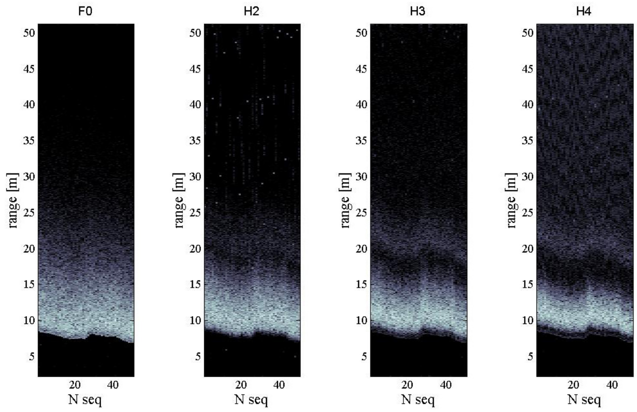

Figure 4. Waterfall of data along 50 pings (x axis) for the first four harmonics.

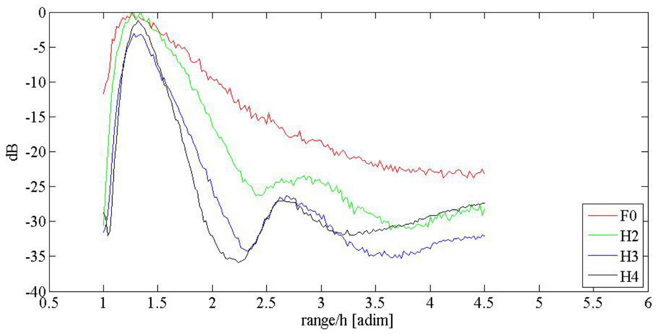

Figure 5. Mean harmonic response versus the ratio range/height, computed with the data displayed in Fig. 4.

Acknowledgments

This project has been funded by IFREMER.

References

[1] F. Parthiot, E. de Nanteuil, F. Merlin, B. Zerr, Y. Guedes, X. Lurton, J-M. Augustin, P. Cervenka, J. Marchal, J-P. Sessarego, RK. Hansen, “Sonar detection and monitoring of sunken heavy fuel oil on the seafloor. NOSCA”, Proceedings Interspill conference, Trondheim, 14-17 June 2004.

[2] J.A. Shooter, T.G. Muir, D.T. Blackstock, “Acoustics saturation of spherical waves in water”, *J. Acoust. Soc. Am*. 55, 54-62 (1974).

[3] B. Ward, A.C. Backer, V.F. Humphrey: Nonlinear propagation applied to the improvement of resolution in diagnostic medical ultrasound. *J. Acoust. Soc. Am.* 101, 143-154 (1997).

[4] M.F. Hamilton, D.T. Blackstock, *Nonlinear Acoustics*, Academic Press, Texas, 2002.

[5] D.T. Blackstock: Generalized Burgers equation for plane waves, *J. Acoust. Soc. Am*., 77, 2050-2053 (1985).

[6] R.E. Francois, G.R. Garrison, Sound absorption based on ocean measurements: Part II:Boric acid contribution and equation for total absorption. *J. Acoust Soc.Am.*, 72, 1879-1890 (1982).

[7] L. Di Marcoberardino, J. Marchal, P. Cervenka, Nonlinear multi-frequency transmitter for seafloor characterization, *Acta Acustica / Acustica*, 97, 202-208 (2011).

[8] L. Di Marcoberardino, J. Marchal, P. Cervenka, Nonlinear multi-frequency generation for underwater application, submitted in Applied Acoustics.